Polytechnic University of Turin
Master's Degree Program in Aerospace Engineering
Academic Year 2022/2023

Politecnico di Torino
1859

# Designing a support for an antenna for aerospace applications using the LB-PBF additive manufacturing technology

*Federico Cocuzza Santuccio*

# Contents

# List of Figures

# Chapter 1

# Design of a support for an antenna for aerospace applications

## 1.1 Specific instructions on the object to be designed

In this exercise, the design of a support for an antenna to be mounted on a satellite (Figure 1.1a) operating in Low Earth Orbit (LEO) was requested. This support must be capable of withstanding the forces experienced during the launch phase and maintaining the antenna stable during the satellite's operation. The satellite will be part of a constellation of 120 other satellites that will be launched over the course of the year using *SpaceX's Falcon 9* launcher. For the launch, the satellite will be positioned vertically inside the payload as shown in Figure 1.1b. In order to ensure the correct functionality of the system, it is necessary to design a robust and reliable support that can withstand the mechanical and environmental stresses present in LEO.

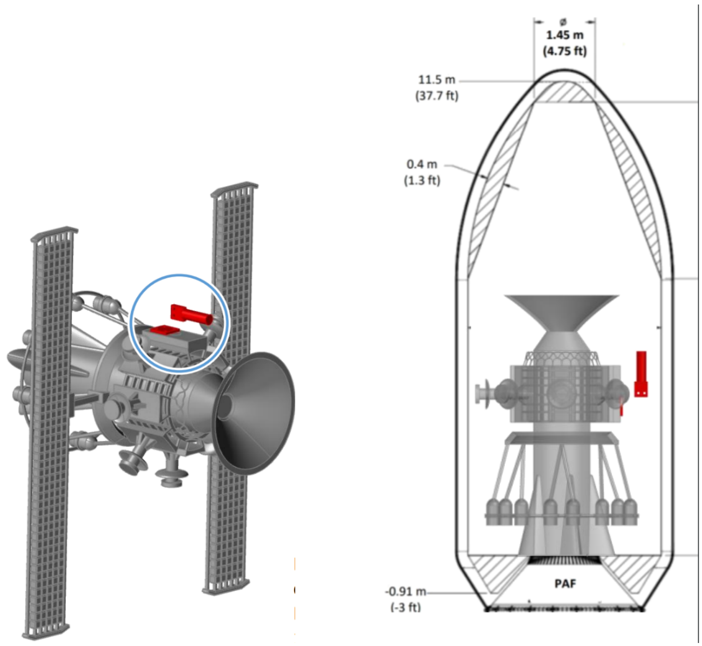


(a) (b)

Figure 1.1

The support to be constructed will have a wide range of shapes and design space; however, it must be connected to both the satellite and the antenna using two specific plates. M8 type bolts will be used for the connections. The antenna will be attached to the rectangular plate, considering that its center of gravity is located at a distance of 250 mm from it, with an approximate mass of 6 Kg.

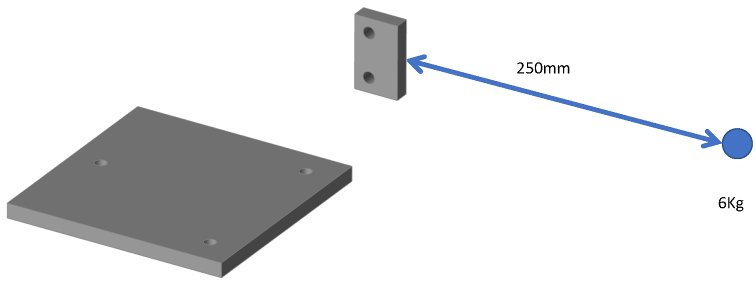


Figure 1.2

## 1.2 Load Conditions

The load conditions are defined based on the *Falcon 9* launcher usage guidelines. During the launch phase, the support will need to withstand a series of inertial loads:

- Axial Load 1: 8.5g
- Axial Load 2: -4g
- Lateral Load: 3g
- Combined Load: 8.5g axial and 2g lateral

Furthermore, during the orbital phases, it will need to withstand thermal loads:

- Maximum operating temperature: 150°C
- Minimum operating temperature: -80°C

## 1.3 Objectives

During the various loading phases to which the component will be subjected, a series of constraints must be met during the design phase.

1. **During Launch**
   - Minimum safety factor for launch loads: 2
   - Maximum displacement (in magnitude) for the entire component: 1 $mm$
   - First natural frequency greater than 15 $Hz$
   - Ensure that the structure can survive an acceleration of 2g for $10^6$ cycles
2. **In Orbit**
   - Thermal load resistance ensuring a safety factor greater than 3
   - Antenna pointing error less than 1°

## 1.4 Component Development

### 1.4.1 Material Selection

The material selection for the support was carried out using the *Granta Edupack* software, which allowed us to significantly narrow down the list of materials to consider. The alpha-beta titanium alloy, *Ti-6Al-4V*, was chosen for its high mechanical properties, its ability to operate within the required temperature range, and its compatibility with the chosen production process, i.e., Laser Beam Powder Bed Fusion (LB-PBF). Using Ashby diagrams, we identified materials that met the requirements of mechanical strength and appropriate density. In particular, we opted for a material that is robust under launch loads but with reduced weight to lower launch and production costs.

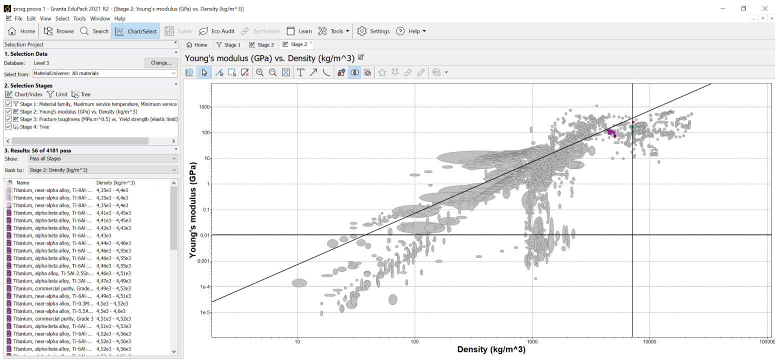


Figure 1.3: Ashby Diagram, Young's Modulus (E) - Density ($\rho$)

In the second Ashby diagram, we have correlated the yield strength of materials with their fracture toughness. These two mechanical properties were chosen considering the need to obtain a component that does not undergo plastic deformation during launch and under the cyclic loads it will experience. Additionally, it is important to ensure that the component does not have internal defects, such as cracks, as this could lead to uncontrolled propagation of such defects during the operational life of the piece.

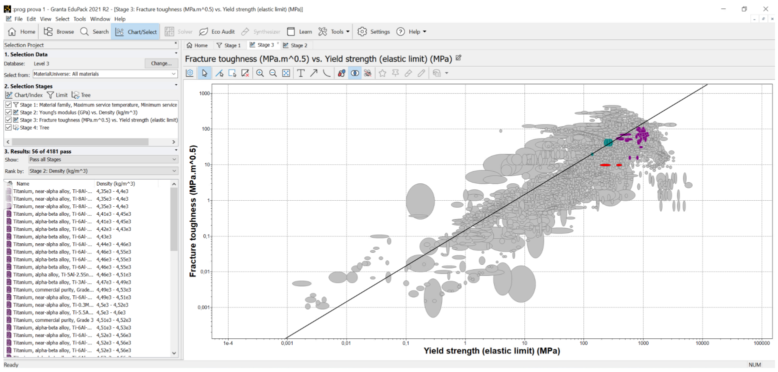


Figure 1.4: Ashby Diagram, Fracture Toughness - Yield Strength ($\sigma_y$)

Finally, we used the Ashby lines to maximize Young's Modulus and Yield Strength, and to minimize Density and Fracture Toughness. This allowed us to identify 56 materials that were theoretically suitable. Subsequently, we analyzed datasheets of commonly used materials in the aerospace industry, excluding some aluminum and nickel alloys due to issues related to high-temperature resistance and density. In the end, we chose the *Ti-6Al-4V* alloy.

### Ti-6Al-4V Alloy

Below is a summary table of the main technical characteristics of the chosen material:

| **Properties** | **Value** |
|---|---|
| Density | $4.43 \cdot 10^3 Kg/m^3$ |
| Young's Modulus | 113-115 GPa |
| Yield Strength | 786-898 MPa |
| Fracture Toughness | $114 MPa \cdot m^{0.5}$ |
| Fatigue $10^7$ cicles | 634 MPa |
| Maximum Operating Temperature | 400°C |

Table 1.1

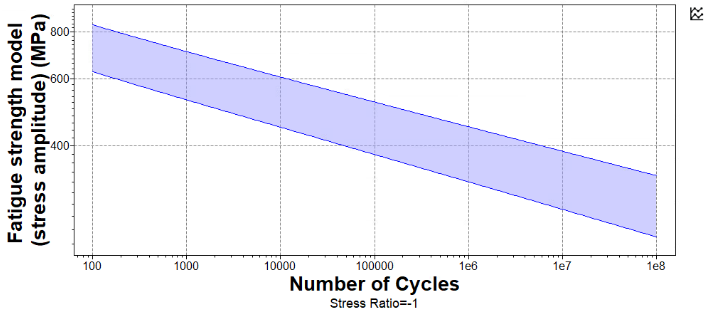


Figure 1.5: Fatigue Strength - Number of Cycles

## 1.5 Component Design

The components designed using the *Altair Inspire* software were developed using two different design approaches. According to the first approach, a broad design space was defined and subjected to several optimization iterations in order to achieve a streamlined and optimal configuration for the component in question. On the other hand, for the second approach, a more confined design space was established, consistent with the conception of the desired final support. Subsequently, the project conceived in this way was optimized and modeled to obtain a geometry suitable for additive manufacturing and meeting the specific requirements.

During the creation of the first design space, we defined four different loading conditions to simulate the stresses the component will undergo during its operational life:

- The loads (in g) provided by the loading conditions.
- The chosen supports in this case are bolts anchored to the satellite plate.

The antenna was connected to the support through its respective plate using 2 bolts, and it was simulated using a concentrated mass of 6 $kg$ located at its center of gravity, 250 $mm$ away from the plate.

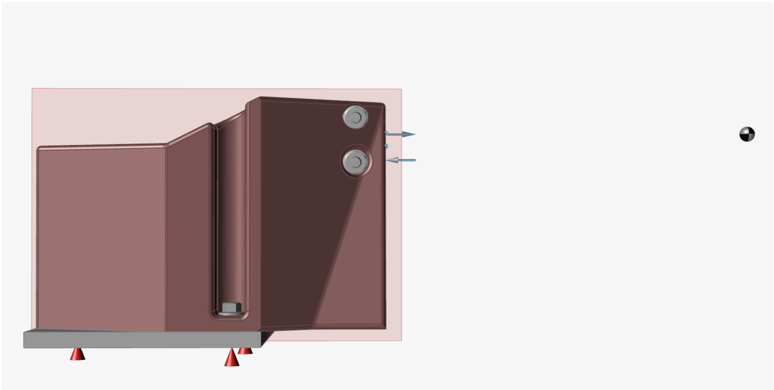

Figure 1.6

## 1.6 Design 1

For the creation of the first design, an initial geometry with a significant bulk was developed. Subsequently, through a series of optimizations aimed at minimizing the component's mass, a result was achieved with a 40% reduction compared to the initial volume. Thanks to this optimization, the design space was significantly reduced, eliminating parts that proved to be superfluous for the realization of the component.

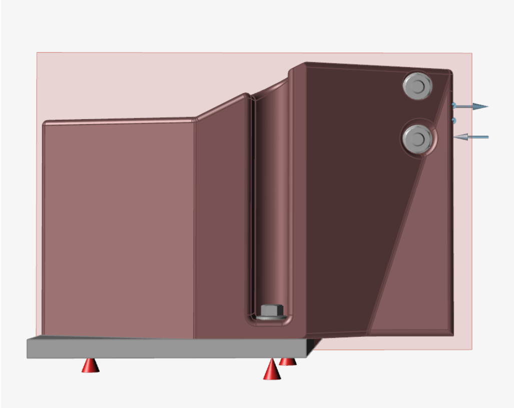

(a)

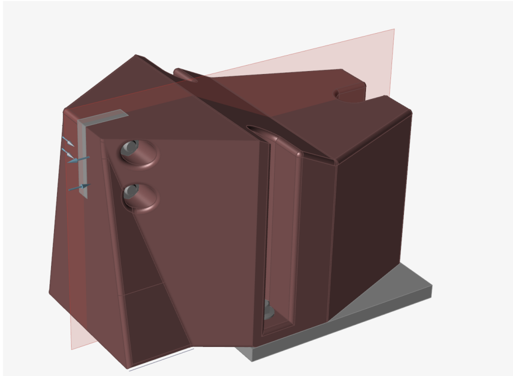

(b)

Figure 1.7: Initial Design Space for Design 1

Starting from the new design space, an initial optimization was performed with the goal of maximizing stiffness and reducing volume by 65%. Subsequently, through a *Polynurbs* adaptation with 1500 parts, a relevant geometry for the project was obtained. However, considering the relatively high mass of the component, approximately 6 $kg$, it was decided to proceed with further optimization.

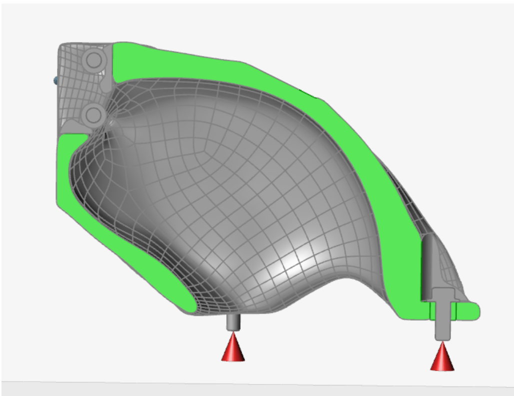

(a)

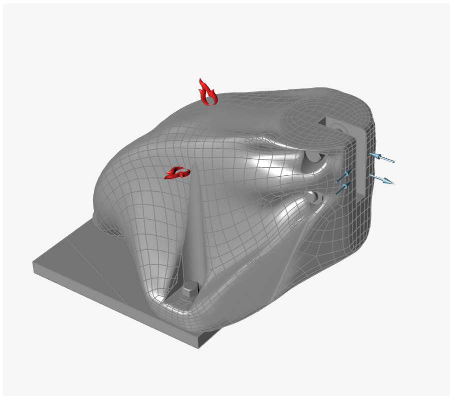

(b)

Figure 1.8: First Optimization for Design 1

By adopting a second optimization phase aimed at maximizing the stiffness of the component under examination, it was possible to significantly reduce the volume of the object by about 80%. This optimization process resulted in a streamlined and lightweight piece, which, subsequently adapted through the *Polynurbs* command with 1000 faces, represented the first final design subject of the investigation.

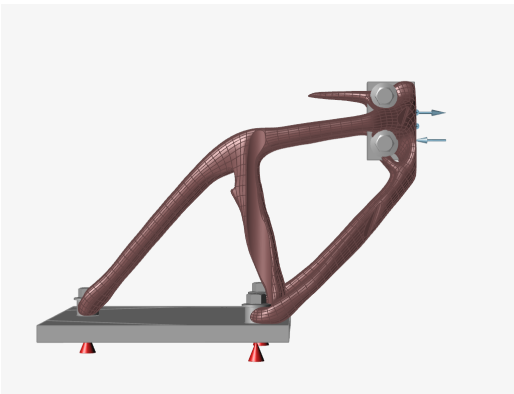

(a)

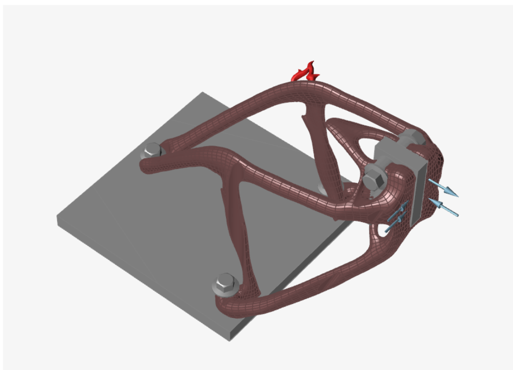

(b)

Figure 1.9: Second Optimization for Design 1

The final mass of the component is 478 $g$.

### 1.6.1 Analysis

The following analyses have been conducted:

1. **Static Analysis**: subjecting the component to launch loads in g
2. **Thermal Analysis**: subjecting the component to two temperature conditions
3. **Normal Modes Analysis**: to find the first natural frequency
4. **Buckling Dynamic Analysis**

#### 1. Static Analysis

It can be observed from the analysis data that for each loading condition, the maximum displacement is always less than 1 mm, and the safety factor is always greater than 2, thus meeting the predetermined design objectives. In the images provided below, you can observe the minimum safety factors for the four loading conditions. Only in condition 3, a minimum safety factor exactly equal to 2 is recorded. However, upon analyzing the points characterized by this value, it is observed that this does not pose a problem for the realization of the component.

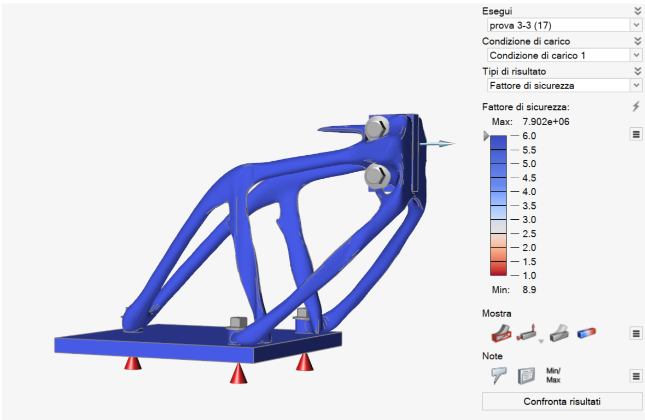


(a) Loading Condition 1

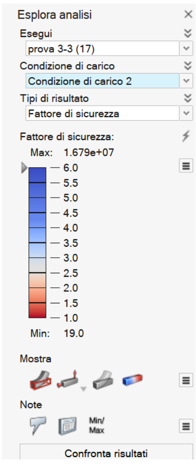


(b) Loading Condition 2

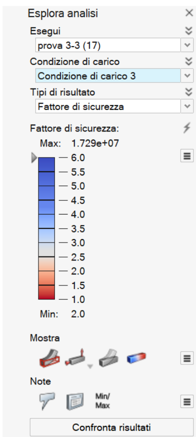


(c) Loading Condition 3

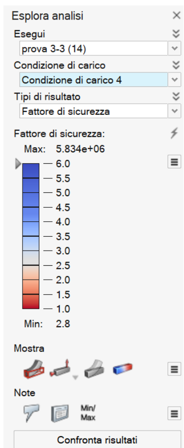


(d) Loading Condition 4

Figure 1.10: Static Analysis for Design 1 - Minimum Safety Factor

Below are the data regarding the maximum displacements for the four different loading conditions. It can be noted that in all cases, the set goals of a maximum of 1 mm displacement have been achieved.

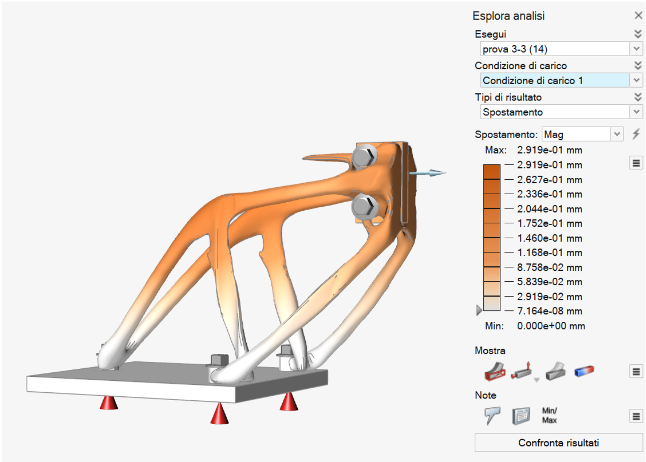


(a) Loading Condition 1

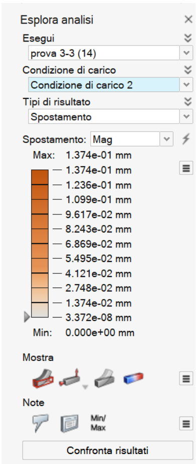


(b) Loading Condition 2

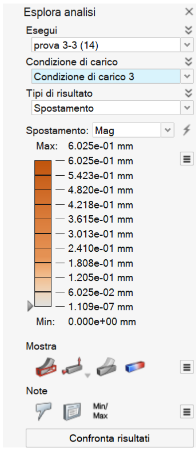


(c) Loading Condition 3

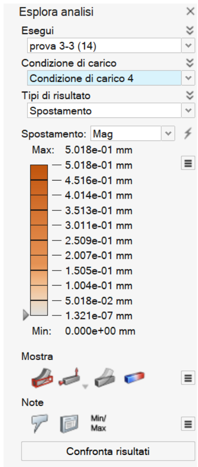


(d) Loading Condition 4

Figure 1.11: Static Analysis for Design 1 - Maximum Displacement

**2. Thermal Load Analysis**

1. **Thermal Load - Minimum Temperature ($-80°C$)**
   From the thermal analysis, it is evident that in these conditions, the component exhibits a high degree of reliability, confirmed by the extremely high average safety factor. Analyzing figure 1.16a, it can be observed that the load factor 3, specified in the design phase, is respected across the entire surface of the component, with the exception of a small area near the bolts where the value drops slightly below the predetermined threshold.

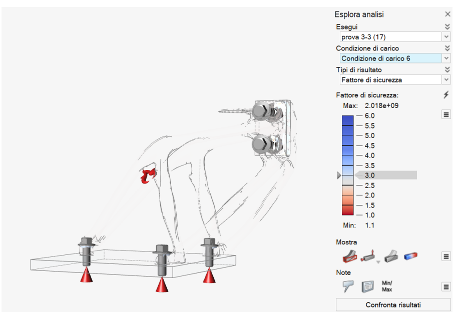

(a)

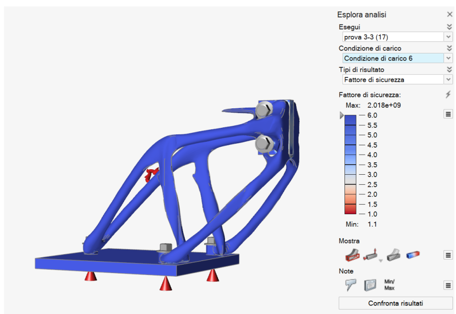

(b)

Figure 1.12: Thermal Load Analysis ($-80°C$) - Minimum Safety Factor

The maximum displacement of the component is less than 1 mm.

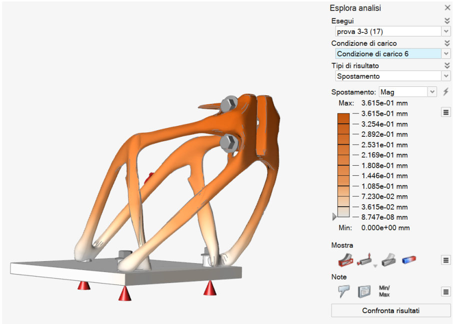


Figure 1.13: Thermal Load Analysis ($-80°C$) - Maximum Displacement

Next, the pointing error was evaluated through trigonometric considerations. To assess the inclination angle of the antenna's center of mass, we verified that its displacement in the three directions was less than 4.3 $mm$. To obtain this data, we performed the following calculation:

$$\Delta_{max} = d \cdot \sin(1°) = 4,36mm \tag{1.1}$$

where $d$ is the distance between the concentrated mass and the component. The observed displacement is 0.089 $mm$, therefore the pointing error is less than 1°.

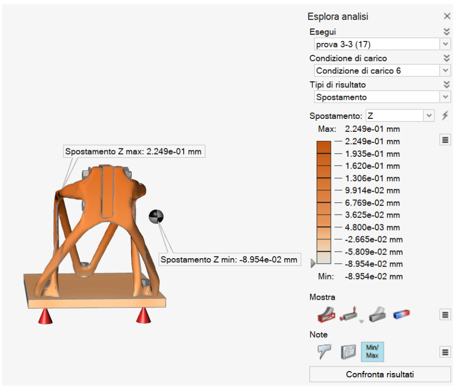


Figure 1.14: Thermal Load Analysis ($-80°C$) - Pointing Error

2. **Thermal Load - Maximum Temperature** ($150°C$)
In this situation, the analysis has shown an overall safe condition, as evidenced by the evaluation of the component's average safety factor (Figure 1.15). However, some critical points have been identified at the attachments with the plates. Nevertheless, it's important to emphasize that, in general, the safety factor of the component is well above the requirements set during the design phase. This result is confirmed by the evaluation shown in Figure 1.15b.

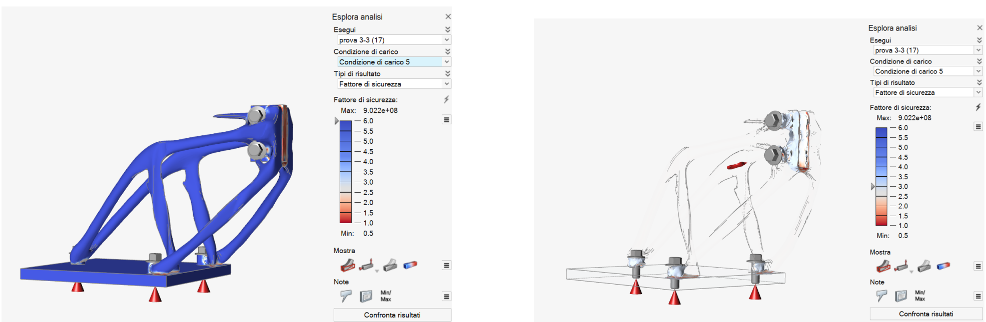

(a) (b)

Figure 1.15: Thermal Load Analysis ($150°C$) - Minimum Safety Factor

The analysis showed that the maximum displacement of the component is less than 1 mm. Additionally, the maximum deviation of the concentrated mass is less than 1°. These results meet the design objectives, ensuring adequate stability of the component and performance in line with the project requirements.

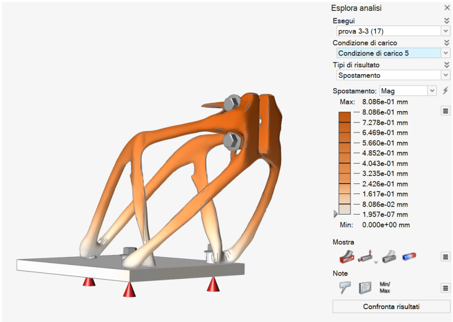


(a) Thermal Load Analysis (150°$C$) - Maximum displacement

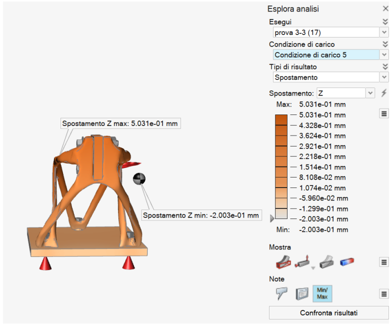


(b) Thermal Load Analysis (150°$C$) - Pointing Error

Figure 1.16

## 3. Modal Analysis

From the normal modes analysis of the component, it can be observed that the primary natural frequency is 29.74 $Hz$, significantly higher than the minimum requirement of 15 $Hz$.

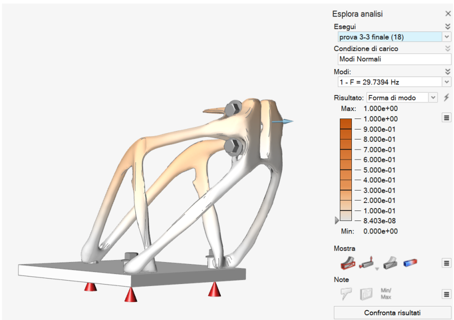


Figure 1.17: Modal Analysis

## 4. Buckling Analysis

Buckling Analysis was performed for the four static loading conditions, and the results are presented in Figure 1.18 and Figure 1.19. For each loading condition, it can be observed that the Buckling Load Factor (BLF) is consistently greater than 1, indicating that there are no instability issues due to buckling.

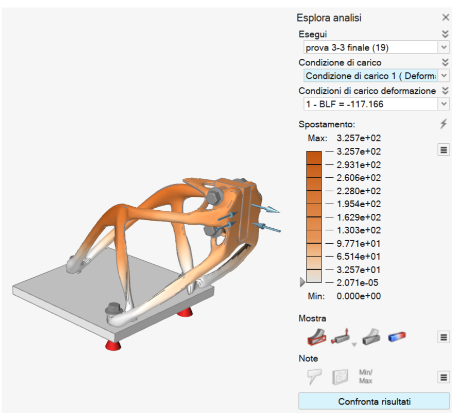


(a) BLF - Loading Condition 1

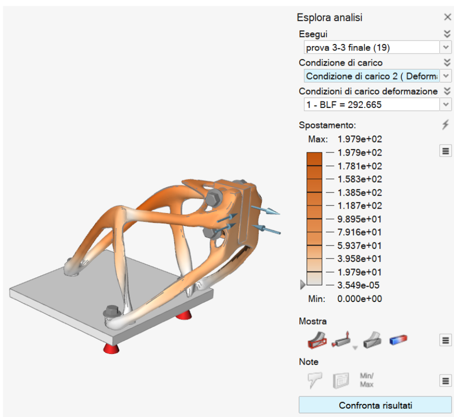


(b) BLF - Loading Condition 2

Figure 1.18

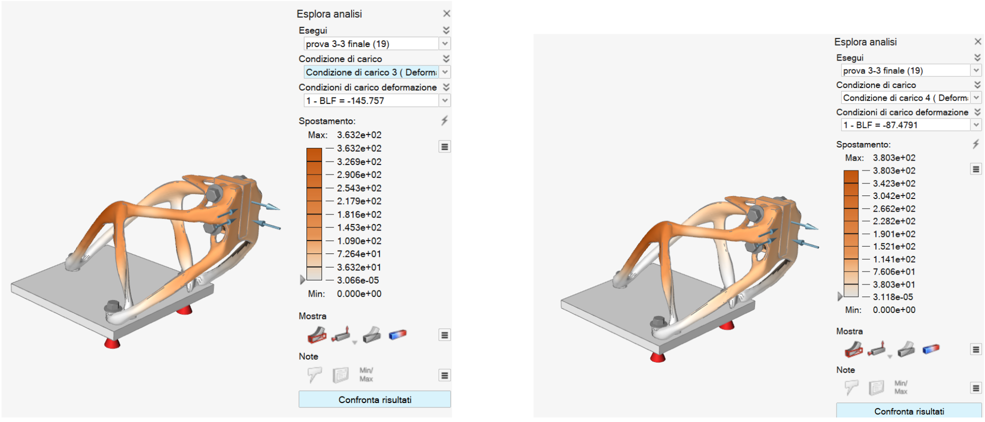


(a) BLF - Loading Condition 3 (b) BLF - Loading Condition 4

Figure 1.19

### 1.6.2 Printing

Using the "*print3D*" feature in *Altair Inspire* software, it was possible to import the designed component and generate the corresponding print using an EOS M 400 printer. Leveraging the flexibility provided by the software, an optimal configuration for the piece's tilt was identified, minimizing the number of supports required and limiting the printing time to an acceptable level. Thanks to this choice, it was possible to plan the production of a total of 120 pieces over the course of a year, ensuring optimal production efficiency.

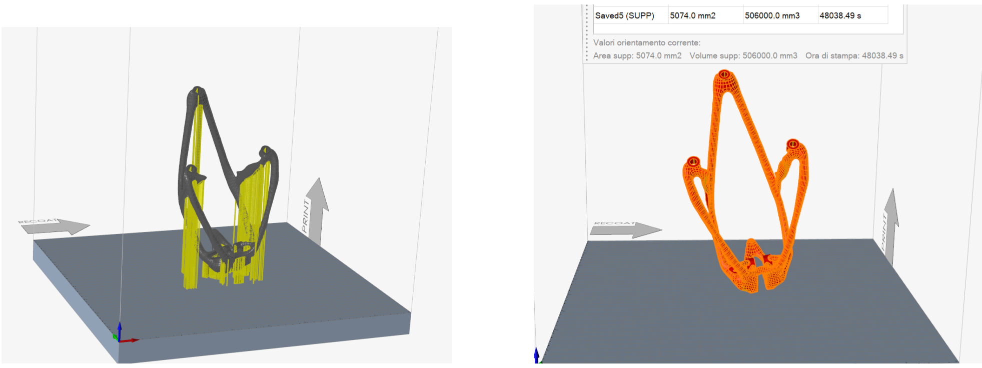

(a) (b)

Figure 1.20: Printing Bed Positioning for Design 1

Through this arrangement of the piece, we achieve:

| | |
|---|---|
| Supports volume | 506000 $mm^3$ |
| Supports area | 5074 $mm^2$ |
| Printing time | 48038s = 13h 21m |

Table 1.2

The size of the printing platform would also allow for the simultaneous printing of 2 or 3 pieces with this inclination, significantly reducing production times and associated costs.

## 1.7 Design 2

For the realization of the second design, a specific design space was outlined to meet the required functional requirements. Although it would be possible to produce the structure depicted in figure 1.21 using conventional processes, an additional optimization of the geometry was carried out in order to reduce its weight and improve its mechanical and thermal performance. This further optimization made the structure more suitable for additive manufacturing.

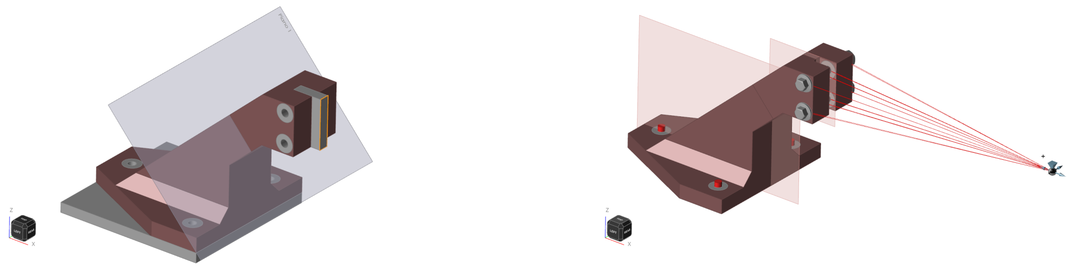

(a) (b)

Figure 1.21: Initial Design Space for Design 2

To improve the component's performance, various optimization strategies were adopted. Firstly, the component was divided into two zones using a plane to create two distinct design spaces (figure 1.21a). Shape controls were implemented to ensure symmetry of the piece in the two zones, along with two fixings to secure the positioning of the antenna's concentrated mass (figure 1.21b). The optimization resulted in an 85% volume reduction of the lower part and a 70% reduction of the upper part. Subsequently, a *Polynurbs* adaptation of the component, consisting of 1500 parts, was performed to obtain the final geometry. These interventions have improved the mechanical and thermal performance of the component as will be shown later.

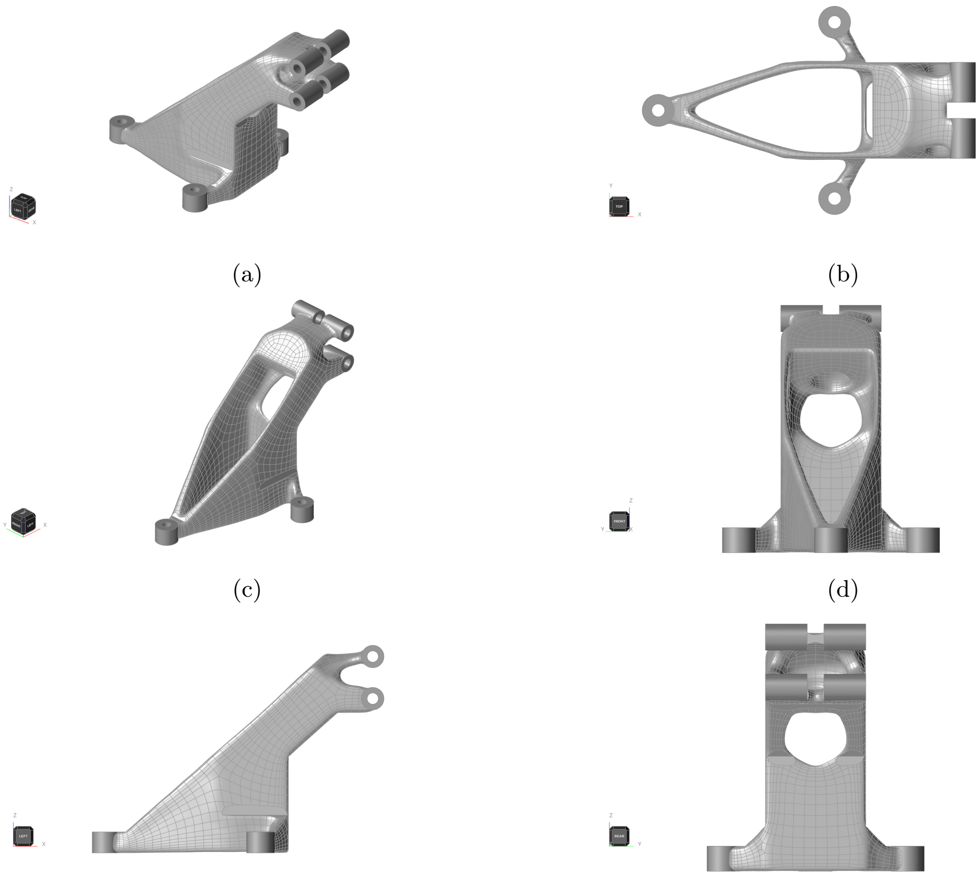

(a) (b) (c) (d) (e) (f)

Figure 1.22: Final Optimization Design 2

The total mass of this design is 850 $g$.

### 1.7.1 Analysis

In this case, the same analyses as in section 1.6.1 were performed:

- **Static Analysis**: subjecting the piece to launch loads in g-force.
- **Thermal Analysis**: subjecting the piece to two temperature conditions.

- **Normal Modes Analysis**: to find the first natural frequency.
- **Dynamic Buckling Analysis**.

### 1. Static Analysis

The following images show the results of the component's displacements obtained through the analysis under 4 different static load conditions. It is clear that in all conditions, the maximum recorded displacements are below the specified limit of 1 mm.

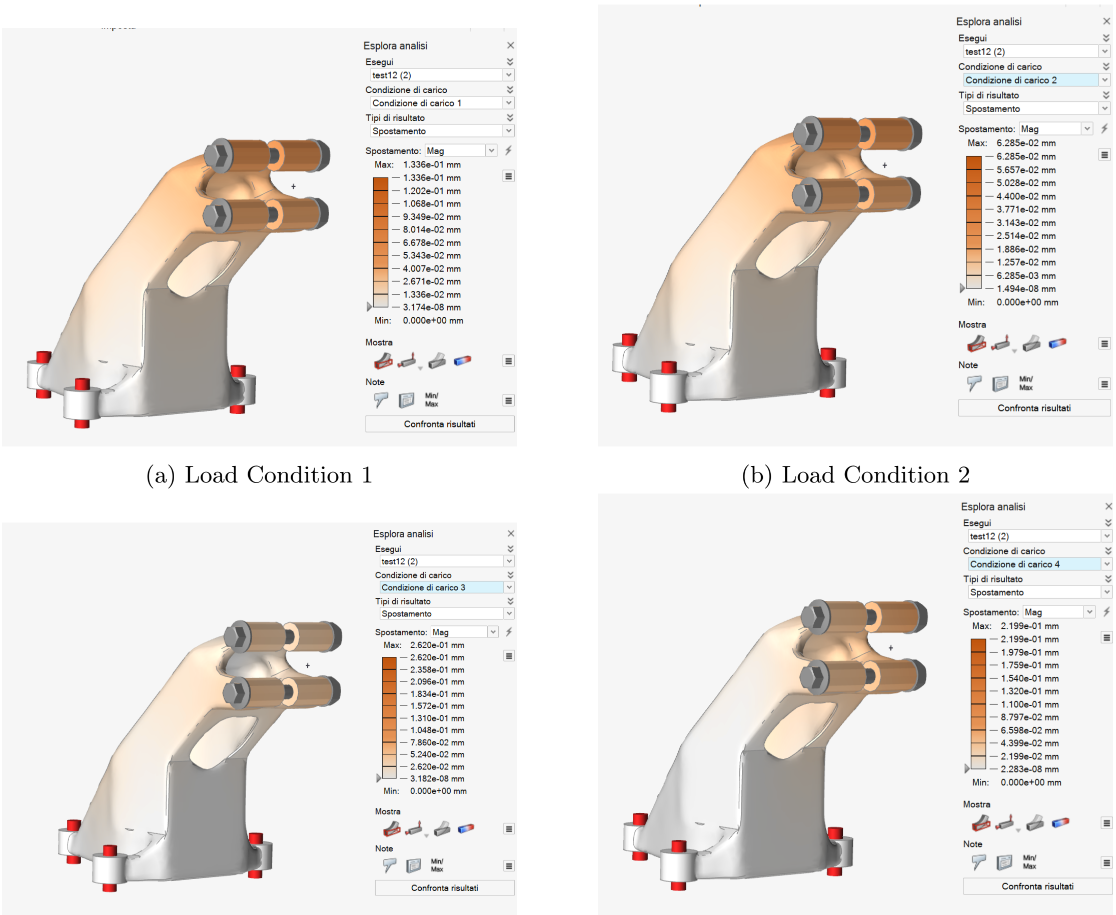


(a) Load Condition 1

(b) Load Condition 2

(c) Load Condition 3

(d) Load Condition 4

Figure 1.23: Static Analysis Design 2 - Maximum Displacement

Below are the minimum safety factor values under the same load conditions. In this case as well, it can be observed that the component meets the required design parameters.

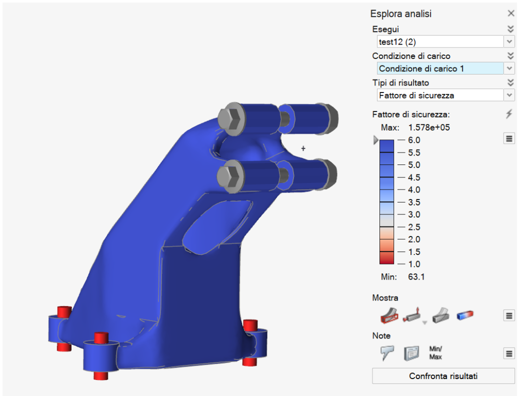

(a) Load Condition 1

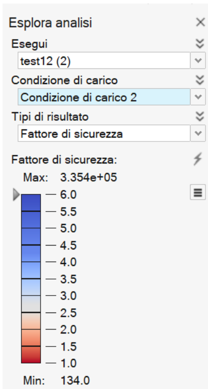


(b) Load Condition 2

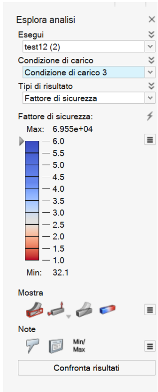

(c) Load Condition 3

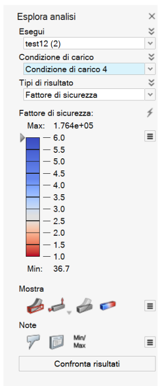

(d) Load Condition 4

Figure 1.24: Static Analysis Design 2 - Minimum Safety Factor

**2. Thermal Load Analysis**

1. **Minimum Temperature Thermal Load** $(-80°C)$ In this condition, it can be observed that the displacement of the component is less than 1 mm, while the safety factor is generally greater than 3 throughout the structure. In particular, although the data displayed in the program may seem to suggest that the minimum safety factor is below the critical threshold, a detailed analysis has demonstrated that in no part of the component does the safety factor fall below this value.

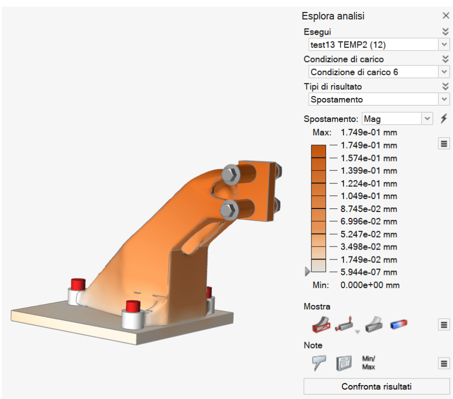

(a) Thermal Load Analysis $(-80°C)$ - Maximum Displacement

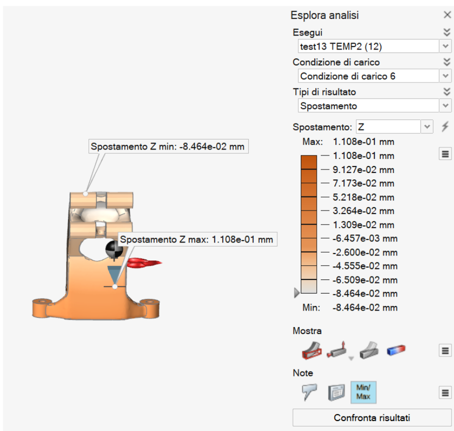

(b) Thermal Load Analysis $(-80°C)$ - Pointing Error

Figure 1.25

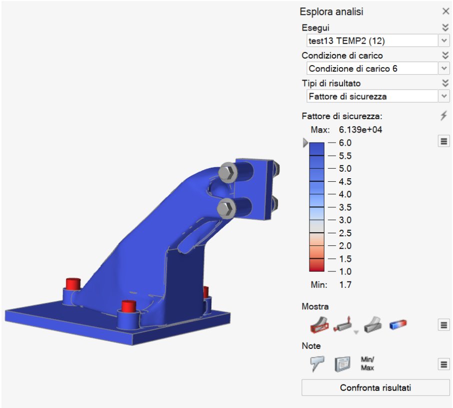


(a) Thermal Load Analysis ($-80°C$) - Safety Factor

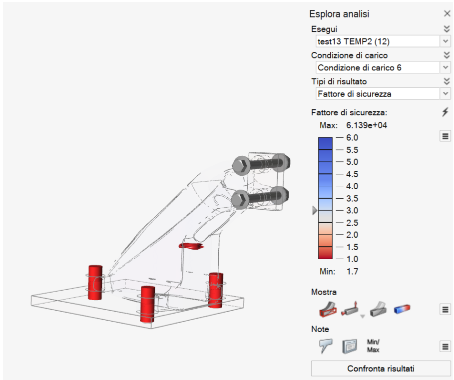


(b) Thermal Load Analysis ($-80°C$) - Safety Factor

Figure 1.26

The pointing error has been evaluated as for Design 1. The displacement of the concentrated mass is 0.11 mm, which is less than 1° as indicated in Figure 1.25b.

2. **Maximum Temperature Thermal Load** ($150°C$) In this condition, it has been observed that the component has a maximum displacement of less than 1 mm and a safety factor generally exceeding 3 throughout the structure, as in the previous case.

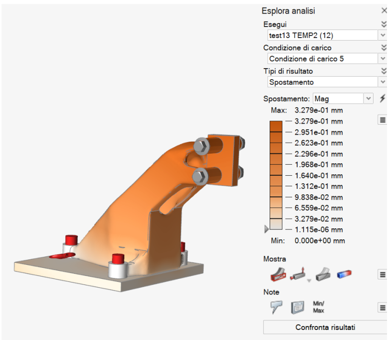


(a) Thermal Load Analysis ($150°C$) - Maximum Displacement

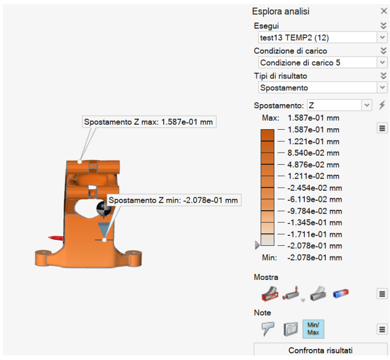


(b) Thermal Load Analysis ($150°C$) - Pointing Error

Figure 1.27

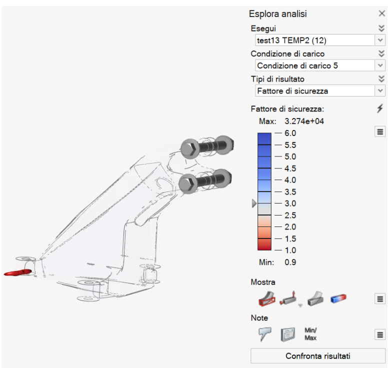


(a) Thermal Load Analysis ($150°C$) - Safety Factor

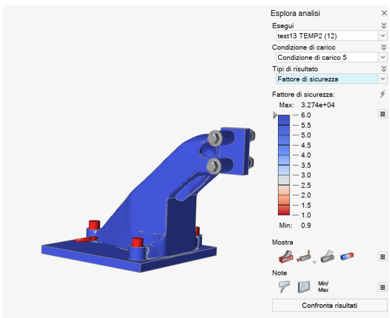


(b) Thermal Load Analysis ($150°C$) - Safety Factor

Figure 1.28

Also in this case, the pointing error is less than 1°. It can be observed in Figure 1.27b that the displacement of the concentrated mass is indeed 0.20 $mm$.

### 3. Normal Modes Analysis

From this analysis, the value of the first natural frequency of the component has been obtained, which is 46.03 Hz. Once again, this exceeds the target value of 15 Hz for this design.

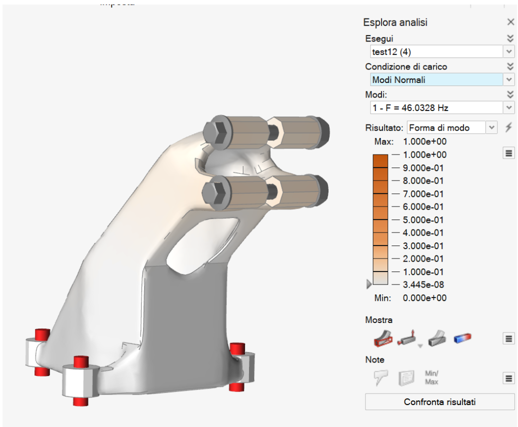


Figure 1.29: Normal Modes Analysis

### 4. Buckling Analysis

Buckling analysis has been conducted for the four static load conditions and the results are shown in the following images. In all load conditions, the *Buckling Load Factor* has been found to be greater than 1, confirming the stability of the component and the absence of deformation phenomena.

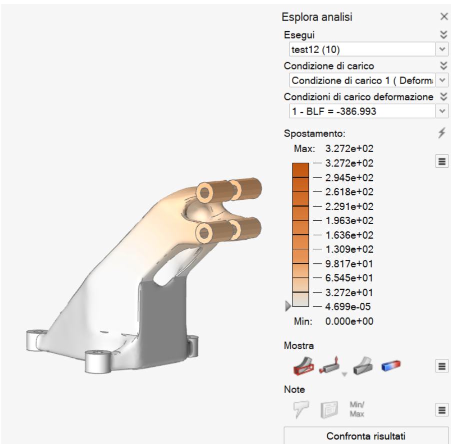


(a) BLF - Load Condition 1

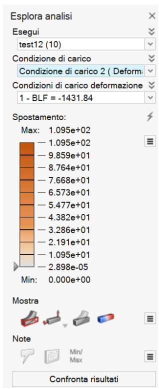


(b) BLF - Load Condition 2

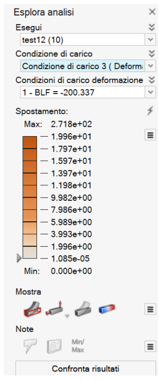


(c) BLF - Load Condition 3

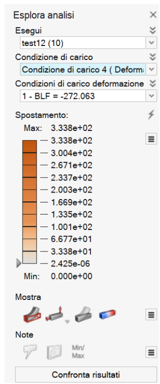


(d) BLF - Load Condition 4

Figure 1.30

### 1.7.2 3D Printing

As with Design 1, we used Altair Inspire's *"print3D"* function to simulate the printing of the component on an EOS M 400 printer. By adjusting the piece's inclination, we found a configuration that required minimal supports and an acceptable printing time to produce 120 pieces in a year.

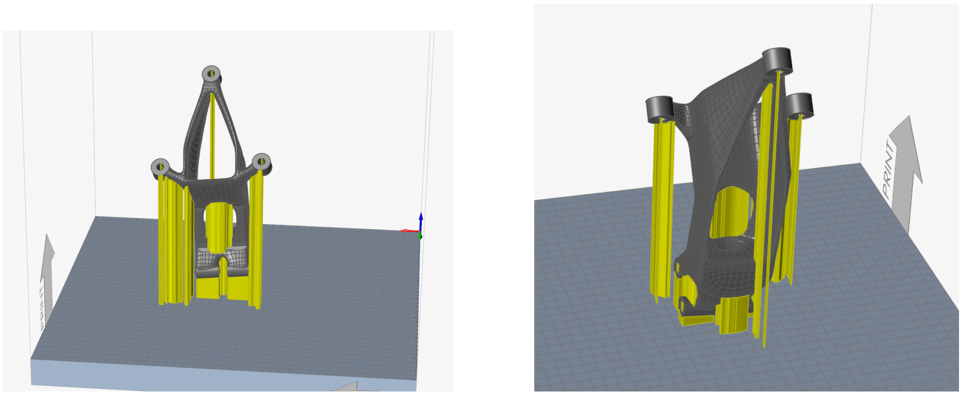

(a) (b)

Figure 1.31: Printing Bed Orientation for Design 2

Through this arrangement of the piece, it is achieved that:

| | |
|---|---|
| Support Volume | 553000 $mm^3$ |
| Support Area | 4993 $mm^2$ |
| Printing Time | 49597s = 13h 46m |

Table 1.3

## 1.8 Comparison between the two designs

Comparing the two designs, it can be observed that both meet the design conditions and objectives. However, Design 2 shows a slight improvement in terms of safety, with higher minimum safety factors for both static load conditions and thermal loads. Nevertheless, the first design has a lower mass (478 $g$ vs. 850 $g$), making it potentially a more cost-effective choice in terms of weight and cost optimization. Additionally, roughly evaluating the printing aspects, Design 1 requires fewer supports and slightly less printing time. Therefore, based on the specific needs of the company, it would be possible to choose a configuration that is either more cost-effective or safer.

## 1.9 Lattice Design

We considered the possibility of making Design 2 in a lattice structure, in addition to the design requirements. Through an optimization process, we were able to achieve a satisfactory result. However, due to the lattice nature of the design, it was not possible to convert it to Polynurbs. This prevented us from performing the necessary analyses to verify the achievement of the design objectives.

(a) (b)

Figure 1.32: Design 3 (Lattice)